

CdS/CdSe Co-Sensitized Solar Cell Prepared by Jointly Using Successive Ion Layer Absorption and Reaction Method and Chemical Bath Deposition Process

Zhou Yang^{1,2}, Qifeng Zhang^{1,*}, Junting Xi¹, Kwang Suk Park¹, Xiaoliang Xu^{2,*}, Zhiqiang Liang¹, and Guozhong Cao^{1,*}

¹Department of Materials Science and Engineering, University of Washington, Seattle, WA 98195, USA

²Department of Physics, University of Science and Technology of China, Hefei, Anhui 230026, China

ABSTRACT

CdS/CdSe quantum dots co-sensitized TiO₂ solar cell was prepared by combining the successive ion layer absorption and reaction (SILAR) method and chemical bath deposition (CBD) method for the fabrication of CdS and CdSe quantum dots, respectively. The effect of CdSe deposition time on the solar cell performance was investigated. It was found that the optimized deposition time for CdSe was 3 h, yielding solar cell power conversion efficiency of 3.3%. The methods introduced in this paper are a simple route for the fabrication of quantum dot-sensitized solar cells with achieving descent power conversion efficiency.

KEYWORDS: Quantum Dot-Sensitized Solar Cell, Titanium Dioxide, Cadmium Selenide, Cadmium Sulfide, Polysulfide Electrolyte.

1. INTRODUCTION

Quantum dot sensitized solar cells (QDSCs) has attracted a lot of attentions during the past several years.^{1–4} QDSCs have a similar configuration to dye-sensitized solar cells (DSCs) containing a layer of oxide (TiO₂, ZnO, SnO₂, etc.) for electron transport, sensitizer adsorbed on the oxide for light harvesting, counter electrode, and electrolyte that is filled in the space between the oxide working electrode and the counter electrode.⁵ Compared with dye molecules used in DSCs, semiconductor quantum dots are advantageous for their tunable band gap as a function of the size of quantum dots,⁶ high extinction coefficients,^{6,7} and large intrinsic dipole moment facilitating charge separation.^{8,9} Furthermore, in view of the multiple exciton generation (MEG) effect in colloidal quantum dots,^{1,10,11} a theoretical photovoltaic conversion efficiency (PCE) of QDSCs has been estimated to be as high as 44%, which is much higher than the Shockley-Queisser limit, ~31%, for single *p-n* junction-based semiconductor photovoltaic devices.¹² Research in the field of QDSCs has been growing very quickly over the past few years. Nowadays,

the highest power conversion efficiency (PCE) of QDSCs is around 4%.^{13–16} Although these values are still lower than those for DSCs, by both drawing lessons from DSC research and adopting much more suitable designs in the fabrication, it is believed that the efficiency of QDSCs could be further improved.

Quantum dots could be grafted on the metal oxide by two different approaches: *in situ* growth and absorption of pre-synthesized quantum dot with or without bifunctional linker. However, the latter always shows relatively low PCE due to the difficulty in achieving sufficient coverage of quantum dots onto the oxide film.^{17,18} Chemical Bath Deposition^{14,19} (CBD) and Successive Ionic Layer Absorption and Reaction^{15,20,21} (SILAR) are methods that have been extensively employed for *in situ* growth of quantum dots on metal oxide. Although, size distribution and particle aggregation are hard to control with these methods, the quantum dot coverage and PCE of cells prepared using these two methods are always better than those of cells produced by a post-adsorption process. CdS/CdSe quantum dots are conventional components used as sensitizer in quantum dot sensitized solar cells.^{13,14,19,22} It has been demonstrated that the CdS layer, the quality of which has an important impact on the solar cell performance, serves as both seed layer to enhance the growth of CdSe quantum dots and an energy barrier layer to reduce

*Authors to whom correspondence should be addressed.

Emails: qfzhang@u.washington.edu (QFZ), xlxu@ustc.edu.cn (XLX), gzc@u.washington.edu (GZC)

Received: 23 February 2012

Accepted: 26 May 2012

recombination between the electrons in metal oxide and the holes in electrolyte.^{19,23} As for the growth of CdS quantum dots, the SILAR method has been extensively adopted to obtain uniform semiconductor coating.^{21,24} However, the preparation of CdSe quantum dots using the SILAR needs to be carried out under inert condition in a glove box^{21,24} or under high temperature.¹⁵ Although CBD method is somewhat time consuming, it can be conducted to deposit CdSe under atmosphere condition.^{25,26}

In this work, the superiorities of SILAR and CBD methods are combined together to create CdS/CdSe co-sensitized QDSCs. The CdS layer and the CdSe quantum dots were deposited by using SILAR method and CBD process, respectively. The purpose of using CdS layer was to enhance the CdSe growth and reduce the deposit time. The effects of CdSe deposition time on the solar cell performance were thoroughly investigated. The samples are named as S1, S2, etc. according to the CBD deposition time for CdSe, as listed in Table I. After the growth of CdS and CdSe, a ZnS passivation layer was coated to reduce the recombination rate.²⁶ Polysulfide electrolyte (1.0 M Na₂S and 1 M S aqueous solution) and Cu₂S counter electrode were used to test the cell performance. A maximum PCE of 3.3% was obtained under AM 1.5 illumination (100 mW/cm²).

2. EXPERIMENTAL DETAILS

The TiO₂ film fabricated on fluorine doped tin oxide (FTO) glass substrate was prepared following the methods previously reported.^{27,28} For the growth of CdS, firstly, the TiO₂ film was immersed into a 0.1 M Cadmium nitrate (Cd(NO₃)₂) methanol solution for 1 min. In this process, Cd²⁺ will absorb on the TiO₂ electrode. Then, the electrode was rinsed with methanol to remove the excess Cd²⁺ and dried in air. Successively, the electrode was dipped into 0.1 M sodium sulfide (Na₂S) solution containing water and methanol (1:1, v/v) for another 1 min. The S²⁻ will react with the pre-absorbed Cd²⁺ to form the CdS. Then, the electrode was rinsed with methanol and dried in air. This procedure was referred to as one

SILAR cycle. Five cycles were employed to deposit suitable amount of CdS on the electrode. CdSe was deposited on the CdS coated TiO₂ electrode by the CBD method as reported in literatures,^{14,19,26} but with some modifications. Briefly, 0.1 M sodium Selenosulphate (Na₂SeSO₃) aqueous, 0.1 M cadmium acetate (Cd(CH₂COO)₂) aqueous solution and 0.2 M trisodium salt of nitrilotriacetic acid (N(CH₂COONa)₃) solution were mixed together with volume ratio 1:1:1. Then the CdS coated TiO₂ electrode was vertically immersed into the solution for CdSe layer deposition under dark condition at 22 °C. A ZnS passivation layer was then deposited on the CdS/CdSe coated TiO₂ electrode by two SILAR cycles with 0.1 M Zinc nitrate and 0.1 M Sodium sulfide aqueous solution as the Zn²⁺ and S²⁻ sources, respectively. The polysulfide electrolyte is composed of 1 M S and 1 M Na₂S in deionized water. A Cu₂S electrode fabricated on brass foil was used as counter electrode of the cell. The preparation of Cu₂S electrode can be described as follows: brass foil was immersed into 37% HCl at 70 °C for 5 min, then rinsed with water and dried in air. After that, the etched brass foil was dipped into the polysulfide solution, leading to a black Cu₂S layer formed on the surface of brass foil.

The morphology was characterized by using scanning electron microscope (SEM, JSM-7000). EDX was employed to analyze the element contents. The photovoltaic properties were measured using an HP 4155A programmable semiconductor parameter analyzer under AM 1.5 simulated sunlight with a power density of 100 mW/cm². The active cell area is 0.32 cm² and the thickness of the TiO₂ film is about 7 μm. Thermal scientific UV-Vis-NIR spectrum meter was used to study the optical absorption properties of the samples.

3. RESULTS AND DISCUSSION

Figure 1 shows the morphology of CdS coated TiO₂ film treated with CdSe layer by varying the CBD deposition time. It can be seen that the surface roughness of the TiO₂ particles gradually increases with the CBD deposition time. That means more CdSe quantum dots attached onto the TiO₂ nanoparticle film as the deposition time increases. From Figure 1(b), it can be clearly seen that a small amount of CdSe quantum dots are deposited on the TiO₂ nano particles. When the CBD growth time is increased to 3 h, almost the entire particle surface turns to be covered by the CdSe quantum dots. As a result, the particles look bigger. Another impact is that the small holes are partially blocked as the CBD time increases. This phenomenon could be evidenced by SEM images shown in Figures 1(e) and (f) and 2. Some particles aggregated together by the CdSe “glue” and look like very large units, especially as seen in Figures 2(c) and (d). From the perspective of cell performance, particle aggregation would reduce the internal area of photoelectrode film for the

Table I. The sensitization parameters of samples.

Sample name	Deposition parameters	
	SILAR cycle for CdS growth	CBD time for CdSe growth (h)
S1	5	0
S2	5	1
S3	5	2
S4	5	2.5
S5	5	3
S6	5	3.5
S7	5	4

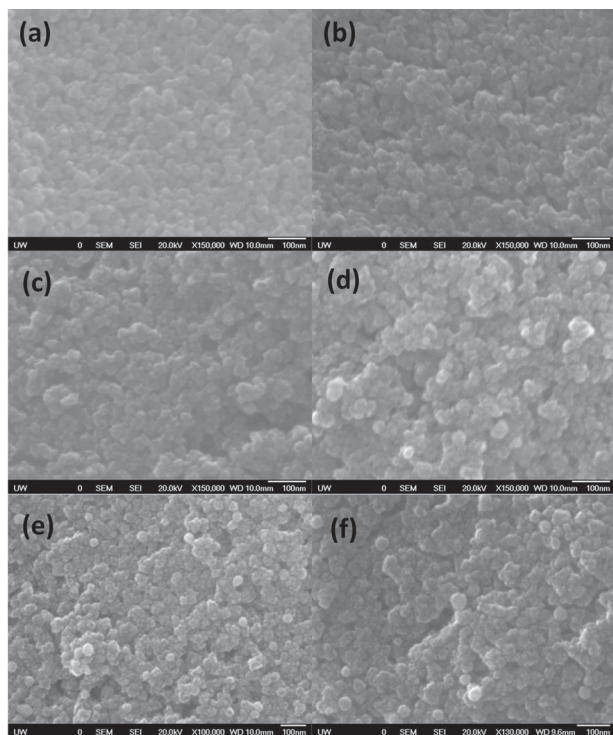


Fig. 1. The SEM images of samples: (a) S2, (b) S3, (c) S4, (d) S5, (e) S6, and (f) S7.

adsorption of quantum dots and hinder the diffusion of electrolyte, leading to a low efficiency.

Figure 3 shows the EDX analysis of Sample S5 and the dependence of weight ratios of Cd to Ti and Se to Ti on the CBD deposition time (inset image). The amount of Cd element present in CdS layer was excluded. When the CBD time is less than 3 h, the Cd/Ti and Cd/Se ratios linearly increase with the growth time. After 3 h, the increment of Cd/Ti and Cd/Se is slow down. However, the color of the reaction solution changed

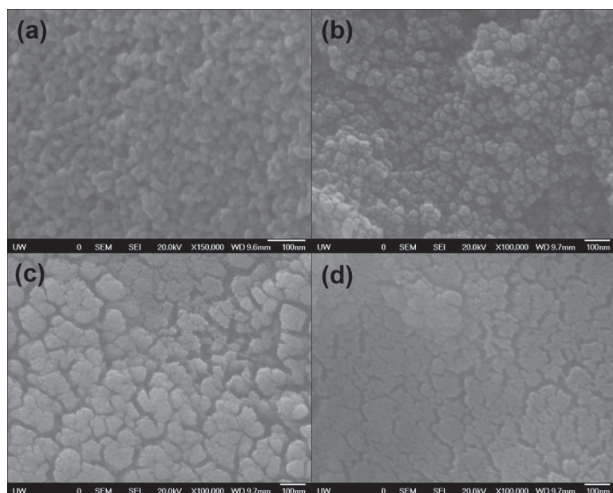


Fig. 2. The cross-sectional SEM images of the samples: (a) bare TiO₂, (b) S5, (c) S6 and (d) S7.

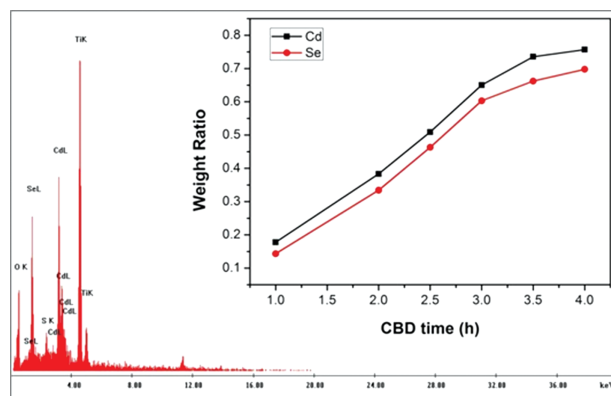


Fig. 3. EDX analysis of Sample S5 and the weight ratios (insert picture) of Cd to Ti and Se to Ti.

dark after we took out the samples, meaning that the CdSe particles in the solution grew larger, and there were abundant ions for the CdSe growth in the reaction solution. The insufficient room for the CdSe growth might be the reason for such an increasing trend for element contents. The element analysis shown in Figure 3 is in agreement with the SEM results (Figs. 1(d), (e) and 2(c), (d)) which show that small holes become blocked with longer CBD process. As reported in Hode's work,¹⁹ the Cd and Se are more or less homogeneously distributed throughout the whole film. Also, by comparative analysis of Figures 1(d), (e) and 2(c), (d) clearly shows that some small holes were blocked with longer deposition, and should be reasonable to the entire film.

Shown in Figure 4 is UV-Vis absorption spectra of the bare TiO₂ film and the quantum dot-sensitized photo-electrodes. Compared with the bare TiO₂ film, the sensitized photo-electrodes can catch photons in the visible region. Since the absorption properties dramatically change with the CBD time, it can be deduced that absorption is mainly controlled by the CdSe layer. In view of quantum confinement effect, the shift of absorption edge of

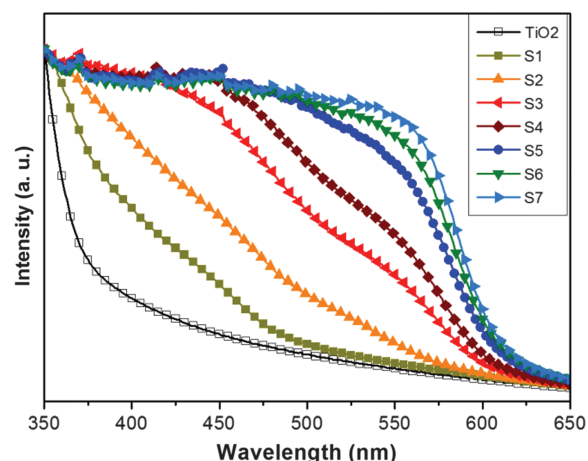


Fig. 4. UV-Vis absorption spectra of a bare TiO₂ film and the TiO₂ films sensitized with quantum dots.

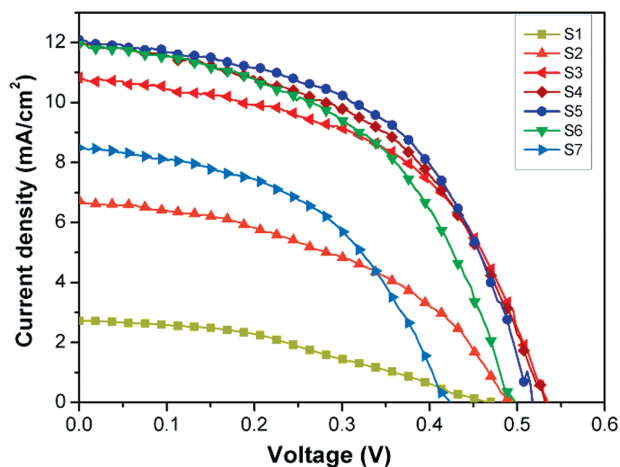


Fig. 5. Current–voltage (J – V) curves for the solar cells corresponding to samples S1 through S7.

the photo-electrode moves to the long wavelength with the increase in CdSe growth period, indicating the increase of the CdSe particle size. The absorption region moves significantly as CBD time is less than 3 h, but the change diminishes while the time surpasses 3 h. This can be ascribed to the gradually saturated room for the CdSe growth. After 3 h, the absorption edge moves to wavelength around 570 nm. The size of the quantum dots can be estimated using the following equation:²⁶

$$\Delta E = E_1 - E_g = \frac{h^2}{8r^2} \left(\frac{1}{m_e} + \frac{1}{m_h} \right) \quad (1)$$

where ΔE is the bandgap shift, E_1 is the bandgap of the quantum dot and could be calculated from the absorption curve (2.18 eV for quantum dots with absorption edge at 570 nm), E_g is the bandgap of the bulk materials (1.74 eV for CdSe bulk material), m_e and m_h are the effective mass of electron and hole, respectively. For CdSe material, the $m_e = 0.11m_0$ and $m_h = 0.44m_0$ and m_0 is the free electron mass. As for $\Delta E = 0.435$ eV, the calculated radius of CdSe quantum dot is 2.81 nm. Therefore, it could be deduced that the holes in TiO_2 film with diameter less than 5 nm may be blocked by the CdSe quantum dot. The electrolyte infiltration will also be hindered to some extent. This result

is in good agreement with the SEM observation as shown in Figures 1(e) and (f) and 2.

Figures 5 and 6 present the photovoltaic performance of the cells with different CdSe deposition time. It could be clearly seen that the CdSe growth time plays a vital role in the cell performance. Rapid increments in both J_{sc} and efficiency during the first 2 h could be observed. This coincides with the growth of the CdSe process, as shown in Figure 2. Following this step, incremental increases of J_{sc} slowed down while V_{oc} showed small signs of decrease. The increase in photocurrent due to quantum dot absorption and the decrease in open circuit voltage due to increased recombination rate (note: the reason will be explained later) compete each other and jointly determine the solar cell efficiency, resulting in a maximum efficiency corresponding to a certain deposition time. From results gathered in this report, a maximum efficiency of 3.3% was attained as for samples with 3 h CdSe deposition time. A similar conclusion was also reported in Meng's work,²⁵ however, the maximum efficiency was achieved at the CBD time of 11 h. The reduction of reaction time in our experiment should be ascribed to the higher reaction temperature, which will accelerate chemical reaction. This trend of PCE increasing and then decreasing with CdSe deposition time could be interpreted as follows. In the first stage, there is an increase in both the amount and size of the quantum dots. That means more photons and the photons with lower energy can be captured by the CdSe sensitizer, as revealed in Figure 4. The absorption intensity increases and the absorption onset shifts to long wavelength. Consequently more electrons will be injected into TiO_2 layer, which makes the J_{sc} increase dramatically and produces a higher V_{oc} . Secondly, as the size of the quantum dots becomes larger, the electron injection process takes more time, explaining why the sensitizer actually absorbs more photons however there is no obvious increment in J_{sc} . Further increasing quantum dot size may increase recombination rate between the electron in quantum dots and the oxidized species in electrolyte. As a result, the V_{oc} decrease a little. Moreover, as more and more CdSe quantum dots are grafted on the TiO_2 surface, the CdSe quantum dots aggregate together and some holes of the film are blocked.

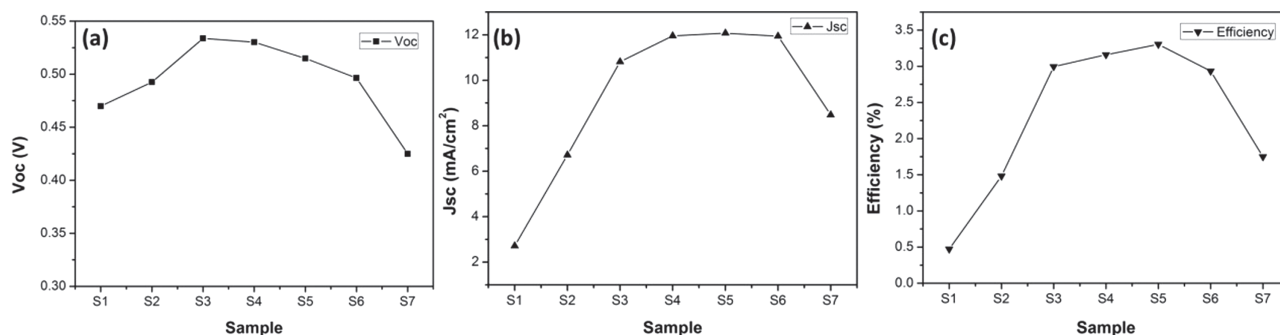


Fig. 6. Trend of photovoltaic parameters for samples S1 through S7.

The photo excited carriers in the inner quantum dot layer could not be extracted effectively. In addition, more and more crystal boundaries are formed as aggregation of the CdSe quantum dots takes place, which will form a lot of recombination centers and increase the loss of the photo generated carriers.^{23, 29} As a result, both the J_{sc} and V_{oc} decrease dramatically as the CBD process longer than a certain time, for example 3 h. The same trend was also reported by Toyoda group.^{23, 29, 30} The poor infiltration of electrolyte, as a result of pores in the nanocrystalline film being blocked, also brings about negative effects on the performance of the QDSCs.

4. CONCLUSIONS

The CdS layer in the CdS/CdSe co-sensitized solar cell was deposited by SILAR method and the CdSe were coated on the CdS layer by CBD method. It was found that the CdSe growth time played an important role in determining the overall efficiency of solar cell. The deposition time affected the thickness of CdSe, which in turn influenced optical absorption and electrolyte penetration of the photo-electrode. An optimized PCE of 3.3% was attained in our experiment with a 3 h CBD deposition for CdSe.

Acknowledgment: This work related to the fabrication and characterization of quantum dot-sensitized solar cells is supported by the U.S. Department of Energy, Office of Basic Energy Sciences, Division of Materials Sciences, under Award no. DE-FG02-07ER46467 (Q.F.Z.). The device fabrication and optimization is also supported in part by the National Science Foundation (DMR 1035196), and the Royalty Research Fund (RRF) from the Office of Research at University of Washington. Zhou Yang would also like to acknowledge the fellowship from China Scholarship Council.

References and Notes

1. A. J. Nozik, *Physica E* 1–2, 115 (2002).
2. P. V. Kamat, K. Tvrđy, D. R. Baker, and J. G. Radich, *Chem. Rev.* 11, 6664 (2010).
3. S. Rühle, M. Shalom, and A. Zaban, *Chem. Phys. Chem.* 11, 2290 (2010).
4. I. Mora-Sero and J. Bisquert, *J. Phys. Chem. Lett.* 20, 3046 (2010).
5. Q. Zhang and G. Cao, *Nano Today* 1, 91 (2011).
6. W. W. Yu, L. Qu, W. Guo, and X. Peng, *Chem. Mat.* 14, 2854 (2003).
7. P. Wang, S. M. Zakeeruddin, J. E. Moser, R. Humphry-Baker, P. Comte, V. Aranyos, A. Hagfeldt, M. K. Nazeeruddin, and M. Grätzel, *Adv. Mater.* 20, 1806 (2004).
8. R. Vogel, K. Pohl, and H. Weller, *Chem. Phys. Lett.* 3–4, 241 (1990).
9. R. Vogel, P. Hoyer, and H. Weller, *J. Phys. Chem.* 12, 3183 (1994).
10. V. I. Klimov, *J. Phys. Chem. B* 34, 16827 (2006).
11. R. D. Schaller, M. Sykora, J. M. Pietryga, and V. I. Klimov, *Nano Lett.* 3, 424 (2006).
12. M. C. Hanna and A. J. Nozik, *J. Appl. Phys.* 7, 074510 (2006).
13. M. A. Hossain, J. R. Jennings, Z. Y. Koh, and Q. Wang, *ACS Nano* 4, 3172 (2011).
14. X. Huang, S. Huang, Q. Zhang, X. Guo, D. Li, Y. Luo, Q. Shen, T. Toyoda, and Q. Meng, *Chem. Commun.* 9, 2664 (2011).
15. Y. L. Lee and Y. S. Lo, *Adv. Funct. Mater.* 4, 604 (2009).
16. M. Seol, H. Kim, Y. Tak, and K. Yong, *Chem. Commun.* 30, 5521 (2010).
17. I. Robel, V. Subramanian, M. Kuno, and P. V. Kamat, *J. Am. Chem. Soc.* 7, 2385 (2006).
18. S. Gimenez, I. Mora-Sero, L. Macor, N. Guijarro, T. Lana-Villarreal, R. Gomez, L. J. Diguna, Q. Shen, T. Toyoda, and J. Bisquert, *Nano-technology* 29, 292504 (2009).
19. O. Niitsoo, S. K. Sarkar, C. Pejoux, S. Rühle, D. Cahen, and G. Hodes, *J. Photochem. Photobiol. A-Chem.* 2–3, 306 (2006).
20. C. H. Chang and Y. L. Lee, *Appl. Phys. Lett.* 5, 053503 (2007).
21. H. Lee, M. Wang, P. Chen, D. R. Gamelin, S. M. Zakeeruddin, M. Grätzel, and M. K. Nazeeruddin, *Nano Lett.* 12, 4221 (2009).
22. V. González-Pedro, X. Xu, I. N. Mora-Sero, and J. Bisquert, *ACS Nano* 10, 5783 (2010).
23. T. Toyoda, K. Oshikane, D. M. Li, Y. H. Luo, Q. B. Meng, and Q. Shen, *J. Appl. Phys.* 11, 114304 (2010).
24. H. J. Lee, J. Bang, J. Park, S. Kim, and S.-M. Park, *Chem. Mat.* 19, 5636 (2010).
25. S. Q. Huang, Q. X. Zhang, X. M. Huang, X. Z. Guo, M. H. Deng, D. M. Li, Y. H. Luo, Q. Shen, T. Toyoda, and Q. B. Meng, *Nano-technology* 37, 375201 (2010).
26. Q. Shen, J. Kobayashi, L. J. Diguna, and T. Toyoda, *J. Appl. Phys.* 8, 084304 (2008).
27. J. Xi, Q. Zhang, K. Park, Y. Sun, and G. Cao, *Electrochimica Acta* 5, 1960 (2011).
28. C. J. Barbé, F. Arendse, P. Comte, M. Jirousek, F. Lenzmann, V. Shklover, and M. Grätzel, *J. Am. Ceram. Soc.* 12, 3157 (1997).
29. S. Hachiya, Y. Onishi, Q. Shen, and T. Toyoda, *J. Appl. Phys.* 5, 054319 (2011).
30. Q. Shen, A. Yamada, S. Tamura, and T. Toyoda, *Appl. Phys. Lett.* 12, 123107 (2010).